J Seismol
https://doi.org/10.1007/s10950-024-10267-8

RESEARCH

Deep learning based earthquake and vehicle detection algorithm

Deniz Ertuncay · Andrea de Lorenzo · Giovanni Costa

Received: 18 September 2023 / Accepted: 8 November 2024

Abstract Seismic recorders register vibrations from all possible sources. Even though the purpose of the seismic instrument is, usually, to record ground motions coming from tectonic sources, other sources such as vehicles can be recorded. In this study, a machine learning model is developed by using a convolutional neural network (CNN) to separate three different classes which are earthquakes, vehicles, and other noises. To do that vehicle signals from various accelerometric stations from Italy are visually detected. Together with the vehicle signals noise and earthquake information coming from Italy are used. Inputs of the database are 10 s long seismic traces along with their frequency content from three channels of the seismic recorder. CNN model has an accuracy rate of more than 99 % for all classes. To understand the capabilities of the model, seismic traces with vehicles and earthquakes are given as input to the model which the model successfully separates different classes. In the case of the superposition of an earthquake and a vehicle, the model prediction is in favor of the earthquake. Moreover, earthquake signals from various databases are predicted with more than 90 % accuracy.

Keywords Machine learning · Traffic monitoring · Vehicle detection · Earthquake detection

D. Ertuncay (✉) · G. Costa
SeisRaM Working Group, Department of Mathematics and Geosciences, University of Trieste, Via Eduardo Weiss 4, Trieste 34128, Italy
e-mail: dertuncay@units.it

G. Costa
e-mail: costa@units.it

A. de Lorenzo
Machine Learning Lab, Department of Engineering and Architecture, University of Trieste, Via Valerio 7/4, Trieste 34127, Italy
e-mail: andrea.delorenzo@units.it

1 Introduction

Seismic instruments record the movement of the ground, which is a superposition of various seismic sources. The sources can be subcategorized into three categories: tectonic, environmental, and anthropogenic. Tectonic sources can be earthquakes and volcanic tremors. Environmental sources are wind (Withers et al. 1996), landslides (Lacroix et al. 2012), thunders (Lythgoe et al. 2021), avalanches (Suriñach et al. 2005) and so on. Cars, trains, and quarry blasts can be examples of anthropogenic sources. Detection of the seismic sources would help us to investigate further the detection of small tectonic events and their locations (Vičič et al. 2019), characterization of features of the ground (e.g., seismic tomography Bianchi et al. 2021), and changes under and above the surface of the earth (Zhao and Rector 2010).

Vehicles can be problematic for seismic monitoring (Allen 1978). Seismometers close to major roads may record vehicles passing continuously. The earthquake detection algorithms can misinterpret these vehi-

Published online: 14 December 2024

cle noises, which can be considered S wave arrival. In case of an earthquake, the presence of a vehicle passing on any station of a seismic network may lead to a miscalculation of the location and magnitude of an earthquake. Hence, seismic network capabilities can be improved by classifying vehicle passages and ignoring them in real-time earthquake monitoring.

Vehicles are not only detected by seismometers but also with other geophysical monitoring tools such as magnetometers (Wang et al. 2017) and acoustic recorders (Liu et al. 2019, Min et al. 2024, Sun et al. 2023, Yuan et al. 2024). To detect the vehicles, different approaches are used, such as frequency-time analysis (Ghosh et al. 2015), wavelet analysis (Sharma et al. 2012), and attenuation analysis (Meng et al. 2021). Dou et al. (2017) used the dispersion curves calculated with distributed acoustic sensing (DAS) recorders. Wavelet analysis are also carried out for DAS sensors (Liu et al. 2019). Machine learning methods are used by using feature extraction by both time and frequency domain information (Ahmad et al. 2022, Hashima et al. 2023, Jakkampudi et al. 2020, Jin et al. 2018, Köse and Hocaoğlu 2023, Uttarakumari et al. 2017, Zhu et al. 2023).

In this study, a machine learning model is developed to identify several features that can be monitored on seismic traces. Three main features are earthquakes, vehicles, and noise. In Section 2, data is introduced, and in Section 3, features of the machine learning model are explained. Results of the study are presented in Section 4, and results are interpreted in Section 5.

2 Data

Data are collected from the National Accelerometric Network (RAN), owned and managed by the Italian Civil Protection Department (Costa et al. 2022, Gorini et al. 2010, Presidency of Counsil of Ministers - Civil Protection Department 1972, Zambonelli et al. 2011). The main purpose of the RAN is to provide information related to ground motion parameters (e.g., PGA, PGV, and PSA) and earthquake physics parameters (e.g., earthquake magnitude). Stations are installed close to the population centres to understand the potential damage of earthquakes. Due to that, seismic traces of the RAN carry information about not only the earthquakes but also the anthropogenic events such as quarry blasts (Gulia and Gasperini 2021; Ertuncay et al. 2024) and vehicles. These non-tectonic sources may have various unwanted effects on seismic monitoring duties.

For instance, quarry blasts may be labelled as earthquakes, which changes the seismicity of the region, thus the seismic hazard of the region (Ghofrani et al. 2019, Gulia and Gasperini 2021). Vehicles may pass near the seismic recorders, which is a common event in RAN since many stations are installed inside public buildings that are generally located near the roads. When a seismic event occurs in a region, a vehicle can pass near a station, which can be interpreted as a part of the occurring event. This leads to an erroneous determination of the epicenter of the event.

Detection of a vehicle can also help to understand the attenuation of the shallow subsurface (Le Gonidec et al. 2021, Meng et al. 2021), the passage of humans (Ketcham et al. 2005) and vehicles (Kalra et al. 2020, Riahi and Gerstoft 2015, Wang et al. 2019) in a particular region.

In vehicle detection, 2 data sources are used, which are the STEAD (Mousavi et al. 2019) database and the RAN. The data set contains three data types: noise, earthquake, and car. Noise data consists of 10000 data points from STEAD and RAN. Earthquake data has 36559 waveforms from events that are publicly available (ran.protezionecivile.it, last access 4th of September 2023). Vehicle waveforms are coming from CNMT, PBN, and PLTA stations in 13 days of 2019 of RAN (Fig. 1), and in total, there is 14885 waveforms.

The starting and ending points of the vehicles are picked via visual inspection. Noise data from RAN are selected from the car-free time ranges from the same dates for vehicles. All signals are detrended, sampling rates are fixed to 100 Hz, 4 corner Butterworth-bandpass filtered between 0.5 Hz and 50 Hz, and are in acceleration domain.

The data length of the waveforms is 10 s. The number is selected by trial and error method between 4 s, 5 s, 10 s, and 20 s. Theoretical P and S wave arrival of earthquakes are calculated, and only the signals with P-S difference less than 7 s are selected. At least 3 s of S wave information is provided to the model, but the selection is essentially made arbitrarily. This is important because the S wave has larger amplitudes than the P wave, and vehicle records have spiky features that can be similar to the nature of the S wave. Earthquakes have magnitudes between M2.5 to M6.0. The frequency

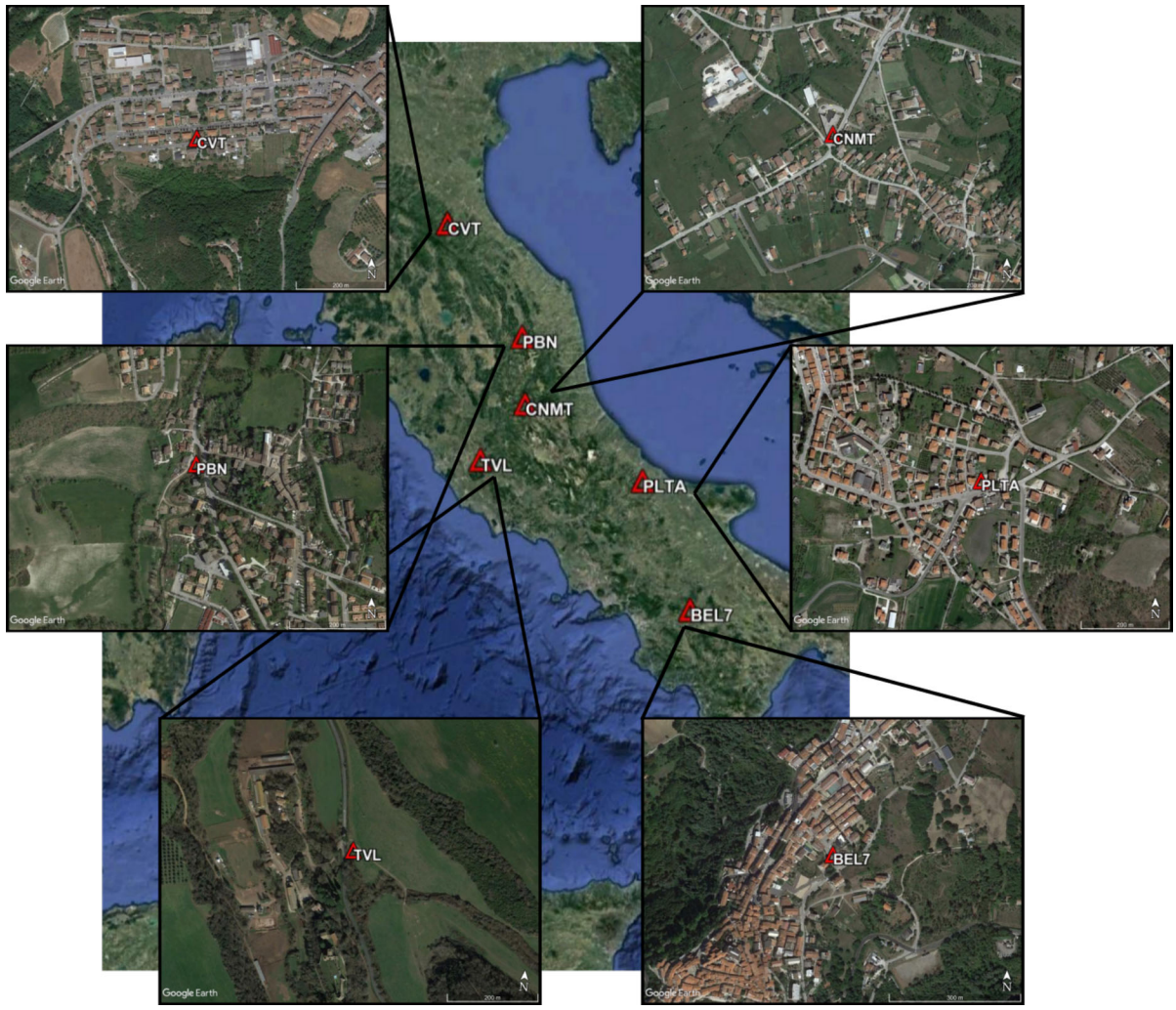

Fig. 1 Locations of the stations (red triangles) that are used in vehicle detection study. Google Earth with satellite information from Landsat/Copernicus are used

content of each class has different information (Fig. 2). Furthermore, Fourier transforms (FFTs) are calculated in real-time for earthquake monitoring purposes (Gallo et al. 2014). If a vehicle duration is shorter than 10 s, the signal is padded with zeros. On the other hand, the first 10 s is selected when it is longer than 10 s.

Both waveforms and FFTs are normalized by using the maximum amplitude in each channel. Peak ground acceleration (PGA) values are similar between earthquakes and vehicles (Fig. 3) depending on the magnitude of the event and the source-to-site distance. Hence, amplitude information cannot be used as an indicator of classification.

3 Method

Our model is based on a convolutional neural network (CNN). The inputs of the model have time, s, and frequency, $\mathcal{F}(s)$, representation of the seismic record. Specifically, the time series input consists of 1000 data points of 10 s signal with 100 Hz sampling rate. The frequency content of the time series includes 500 data points of frequencies up to 50 Hz, with 0.01 Hz interval. The main rationale for using frequency and time series data is to leverage routines already implemented for real-time earthquake monitoring tasks (Costa et al. 2022). Vehicles and earthquakes exhibit distinct char-

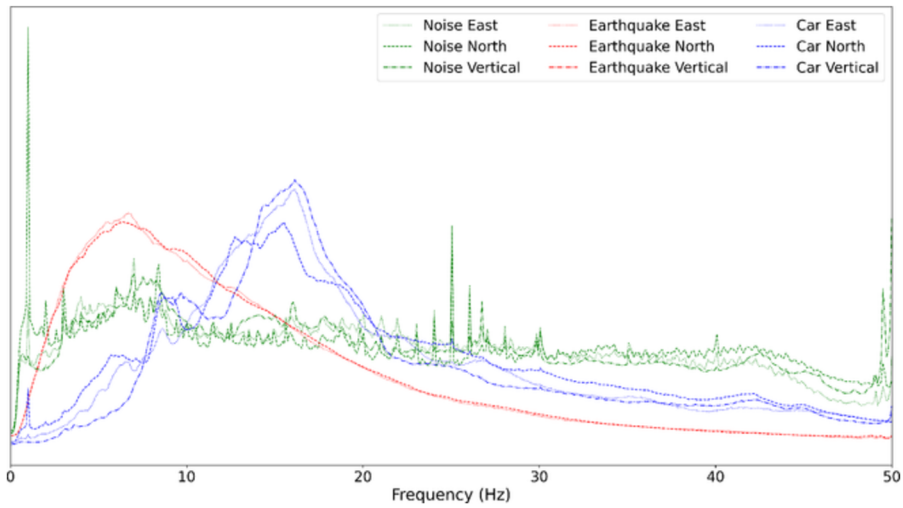

Fig. 2 Averaged frequencies of channels of noise (green), vehicle (blue), and earthquake (red)

acteristics in both time and frequency domains compared to background noise. In the time domain, vehicles produce monochromatic waveforms, while earthquakes have much more complex time signatures that vary based on the epicentral distance. In the frequency domain, the frequency contents of vehicles and earthquakes differ, as depicted in Fig. 2.

The CNN model comprises two convolutional components to handle time and frequency inputs. These input lengths differ, and the CNN model possesses specialized convolutional parts to process them. Given that RAN includes three-component seismic recorders, all components serve as inputs to the CNN, rendering both waveform and FFT inputs multi-channel four 1D convolutional layers, each with 3 channels, interconnected with max-pooling layers, determine the features from the inputs. Subsequently, the extracted information is concatenated and stored as a 1D vector. Densely connect layers and then process this vector to complete the procedure. The network structure is illustrated in Fig. 4. Python packages of Tensorflow (Abadi et al. 2015) and Keras (Chollet et al. 2015) are used to construct the CNN model.

In more detail, both the waveform and FFT components of the CNN consist of 4 layers. These layers have 64, 32, 32, and 16 filters respectively, with kernel sizes of 6, 3, 3, and 3. The max-pooling layers inserted between these convolutional layers possess a size of 4 for the first layer and a size of 2 for the subsequent ones. The activation function employed is the Recti-

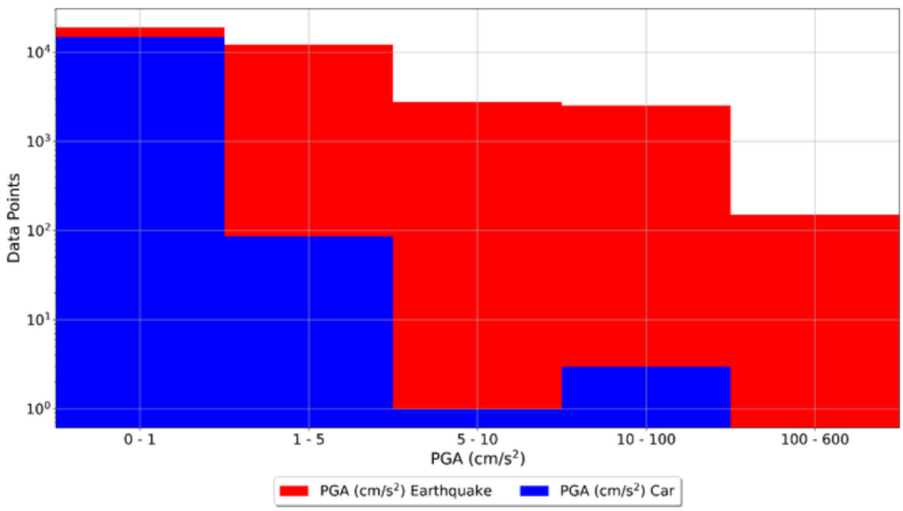

Fig. 3 PGAs of vehicle (blue) and earthquake (red)

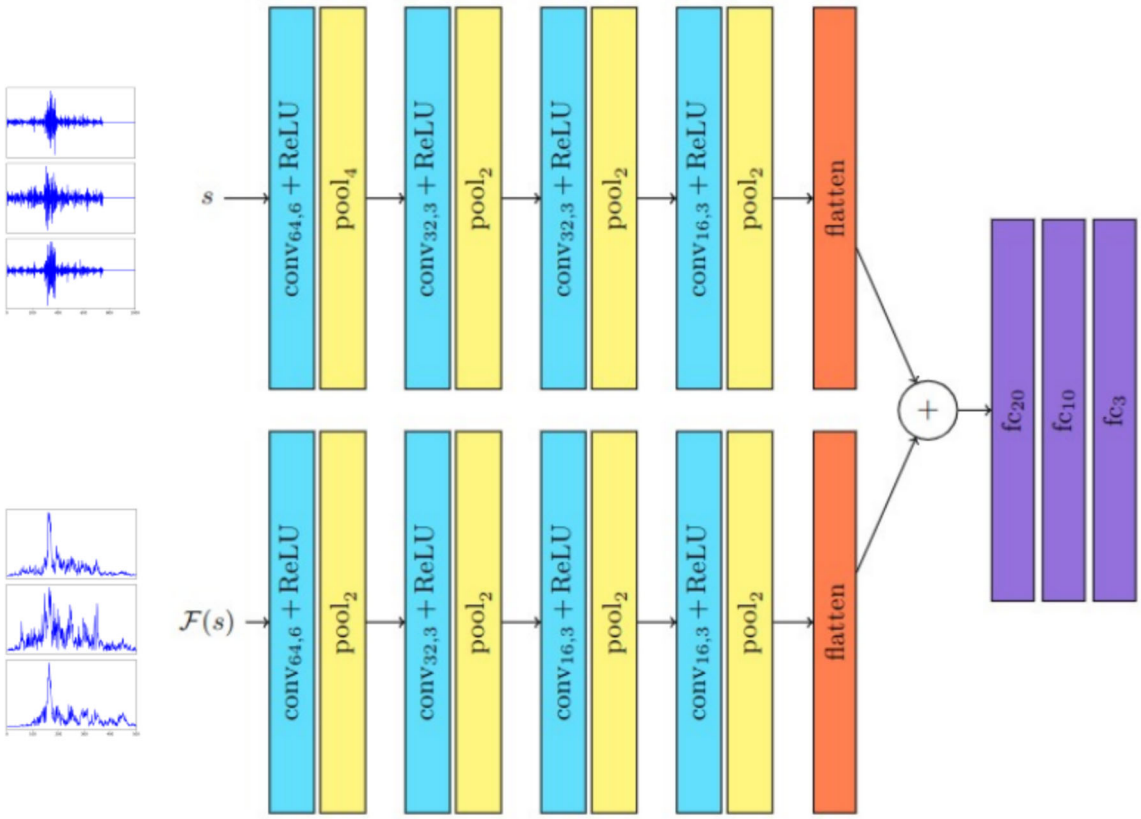

Fig. 4 Convolutional neural network workflow for classification

fied Linear Unit (ReLU), and the initial weights are set using Glorot normal initialization (Glorot and Bengio 2010). Following the concatenation of the aforementioned layers, two fully connected layers with 20 and 10 neurons, respectively, are employed, with both using the ReLU activation function. The concluding layer emits the probability for 3 classes, with the softmax activation function determining the most likely class. The network employs a gradient descent optimizer with a learning rate of 0.01.

4 Results

We employed various metrics to assess our model's performance in signal source identification. These included Cohen's kappa score, the area under the curve (AUC) of the receiver operating characteristic (ROC) results (as shown in Fig. 5), and the confusion matrix. Cohen's kappa score is particularly valuable for multi-class classification problems, especially when the classes are imbalanced. In our case, the classes are noise, earthquake, and vehicle.

$$\kappa = \frac{p_0 - p_e}{1 - p_e} \tag{1}$$

In Eq. 1, p_0 represents the observed accuracy, signifying that the classifier has correctly classified the data throughout the given set. p_e denotes the expected accuracy, which can be interpreted as the total sum of correct and incorrect predictions. The κ value ranges between 0 and 1, with values closer to 1 indicating superior results. We employed a one-vs-rest approach for AUC, wherein each class is evaluated against the rest. AUC values fall between 0 and 1, and predictions approaching 100 % accuracy yield AUC scores closer to one. Additionally, we display the results using a confusion matrix, which offers a summarized view of the model's predictions. For a flawless model, entries in the confusion matrix should align diagonally.

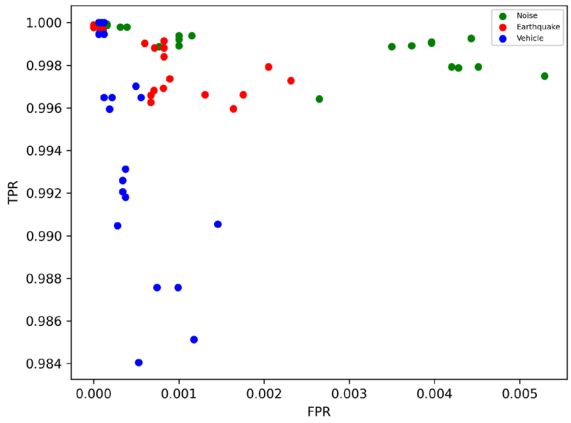

Fig. 5 Receiver operating characteristic performance of developed mode for each class

The model's evaluation was conducted using 4-fold cross-validation, and the results were averaged. To circumvent the potential bias of a "lucky" training set, experiments were repeated 5 times. This resulted in a total of 20 experiments, with 113583 signals for each training fold. Models have trained over 20 epochs, and at the end of these epochs, each model was evaluated using a distinct validation set, comprising 25 % of the database (Table 1). Training was halted if the loss function in the validation set increased for 2 consecutive epochs to prevent overfitting.

For our dataset, the average AUC and κ values across the 20 repetitions were 99.99 % and 99.64, respectively. The average confusion matrix from all repetitions is presented in Table 2. This indicates that our model can accurately classify inputs from each class with a precision exceeding 99 %.

5 Discussion and conclusion

AUC value in vehicle detection shows that the ability of the classifier to distinguish classes is significantly good (99.99 %). Moreover, a high κ value means that our model makes good predictions even though the data is unbalanced between classes (99.64). To see the capabilities of our model, we made predictions on unseen signals from BEL7, CVT, PBN, and TVL stations (Fig. 1). In Fig. 6, an hour-long prediction results can be seen. Waveforms are normalized by using the largest amplitude of each channel for an hour-long data, even though in the prediction process, normalization is done in 10 s inputs. Starting from the beginning of each signal 10 s chunks are retrieved and FFTs are calculated for the prediction. Iteration over data points is done for every 5 s. Predictions of the model are plotted as a line that varies between 0 to 1 which means 0 % to 100 % in terms of prediction for each label.

Due to their relatively long duration, traces with a superposition of multiple vehicles are avoided in the manually detected vehicles. However, in reality, it is a common occurrence. To see the prediction capability of our model in such cases, specific examples are retrieved from the RAN (Fig. 7). As can be seen, our model is capable of successfully detecting these signals as vehicles. Even though seismic traces may change due to amplification or abbreviation, their frequency content still carries information from vehicles. Between 6 s to 15 s in Fig. 7 model prediction returns vehicle output. It is due to the fact that the input takes 10 s long signal, which includes the beginning of the vehicle passage around 17 s.

We also analyzed the signals from the dates earthquake signals were detected. As seen in Fig. 8, our model distinguishes vehicles from earthquakes successfully. The PBN station is chosen as an example to show the model's performance with earthquake and vehicle passing records. The station is next to the road in the village of Pievebovigliana in Central Italy. The recorded earthquake with a magnitude of 2.4 occurred on the 5th of January 2023 at 21:54:44 (UTC) with an epicentral distance 3.71 km. There are 3 vehicles passed near the station before the earthquake, and all the vehicles are successfully labelled along with the earthquake. However, there are several incidents where our model predicts many false earthquakes (Fig. 7).

Table 1 Average of validation data

		Label		
		Noise	Earthquake	Vehicle
Prediction	Noise	23076.60	14.60	11.05
	Earthquake	14.80	9122.05	2.90
	Vehicle	15.15	7.90	3698.20

Table 2 Confusion Matrix

		Label		
		Noise	Earthquake	Vehicle
Prediction	Noise	99.89	0.06	0.05
	Earthquake	0.16	99.81	0.03
	Vehicle	0.41	0.21	99.38

False earthquakes may predicted where vehicles are at present as well as pure background noise. However, in the visual inspection, we realised their occurrence is negligible. The model can be retrained with many earthquake and noise signals to avoid false predictions. However, we used a relatively small dataset to avoid uneven train examples among classes. Furthermore, RAN is already using the earthquake detection routine from Antelope software (Costa et al. 2022) to detect earthquakes, and our model is developed to help the earthquake detection algorithm to exclude vehicles.

Furthermore, we created new sets of data to see the capability of our model in terms of the detection of earthquakes. To do that, we used the Italian seismic dataset for machine learning (INSTANCE, Michelini et al. 2021) and ITalian ACcelerometric Archive (ITACA, Felicetta et al. 2023). From the INSTANCE database, we select 10000 earthquake signals recorded by strong motion stations of earthquake magnitude between $M1$ and $M6$. All data from stations we used in the training and validation process are excluded. Signals have both P and S arrivals registered, and the

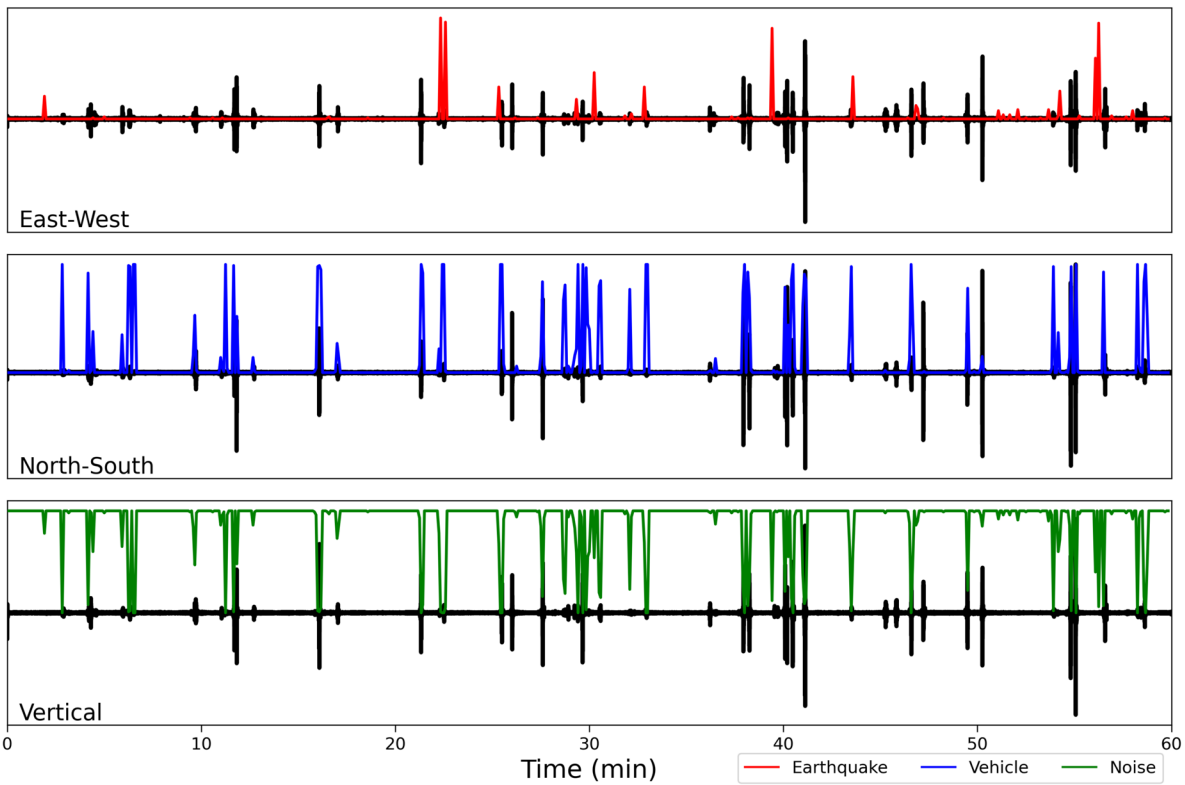

Fig. 6 Model prediction of noise, earthquake, and vehicle classes an hour-long seismic trace vehicle passing recorded at BEL7 station on 20th of January 2023 between 18:00 and 19:00 (UTC). Green, blue, and red lines with dots indicate model prediction for noise, vehicle, and earthquake, respectively. From top to bottom the components are East-West, North-South, and vertical of BEL7 and predictions are plotted on separate channel to increase the readability of the figure

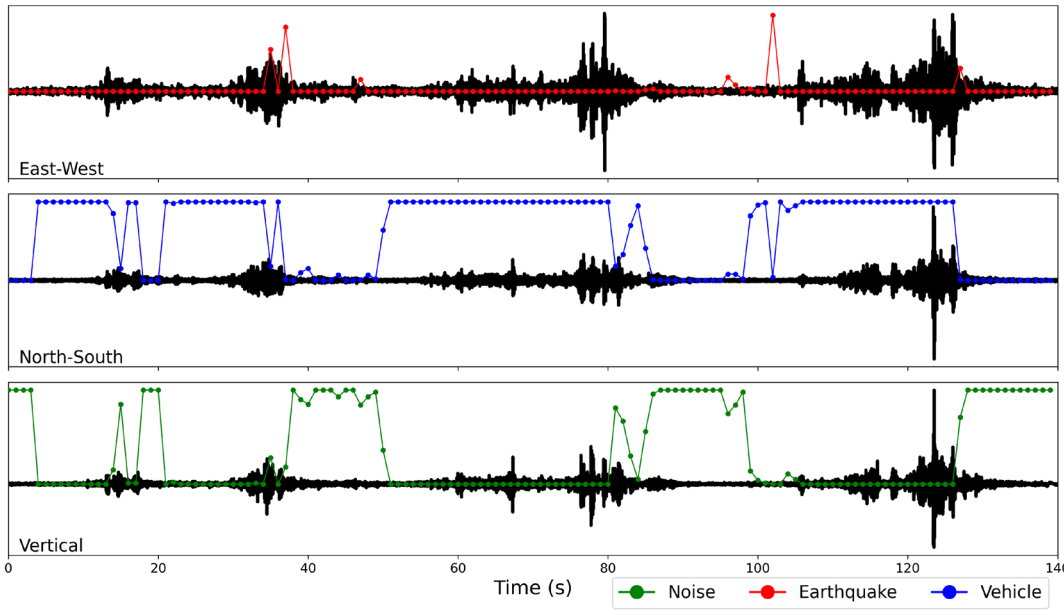

Fig. 7 Model prediction of multiple vehicle passing recorded at CNMT station. Green, blue, and red lines with dots indicate model prediction for noise, vehicle, and earthquake, respectively. From top to bottom, the components are East-West, North-South, and vertical of CNMT, and predictions are plotted on separate channels to increase the readability of the figure

time difference between arrivals is less than 7 s is used. Our model detect earthquakes with 96.15 % accuracy (Table 3). We also retrieve raw acceleration data from ITACA with magnitudes larger than $M3$. All signals that are coming from training and validation are also excluded. We calculate the P and S wave arrival of the signals by using the ray path models of Kennett and Engdahl (1991) and only selected signals with P and S wave arrival less than 7 s. Our model identify 8038 signals out of 9139 signals correctly (accuracy rate: 87.95 %, Table 3).

As a final test of our models, we created an artificial signal by adding up an earthquake and a vehicle on top of each other. The idea behind this is to see the capability of our model when an earthquake and vehicle traces arrive at the recorders simultaneously. To do that, we selected the earthquake trace recorded by CVT station that occurred on 23rd of April 2023 at 16:17:35 (UTC) with magnitude 2.5 and epicentral distance of 17.2 km. PGA of the earthquake for the station is 3.94 cm s^{-2}. TVL station is located 24 km away from Rome, Italy and next to an ST51a regional road with a distance of a couple of meters. The station is inside an electric transformer cabin. A car trace is selected from the 20th of January 2023 at around 17:45 (UTC) and is used for the analysis with PGA of 1.51 cm s^{-2}. The vehicle signal is shifted over the earthquake signal second by second, and in each iteration, model predictions are observed (Fig. 9). Our model returns with the output of the earthquake even though there is a vehicle signal along with the earthquake. The only vehicle output is retrieved in the last iteration (10 s shift), where only a small part of the S wave and coda waves are present. In the training phase, the maximum P-S time difference is selected as 7 s, which means that in some of the earthquake signals, the last part of the S wave and coda waves are not given as input, which can explain why in the last iteration the output is vehicle. One problematic outcome of the model prediction would be its precision. Even though in the input signal there is always a vehicle signal, the prediction of the model is always earthquakes with almost 100 % certainty. This model is developed to help misidentify vehicles as earthquakes; therefore, the prediction satisfies our needs. However,

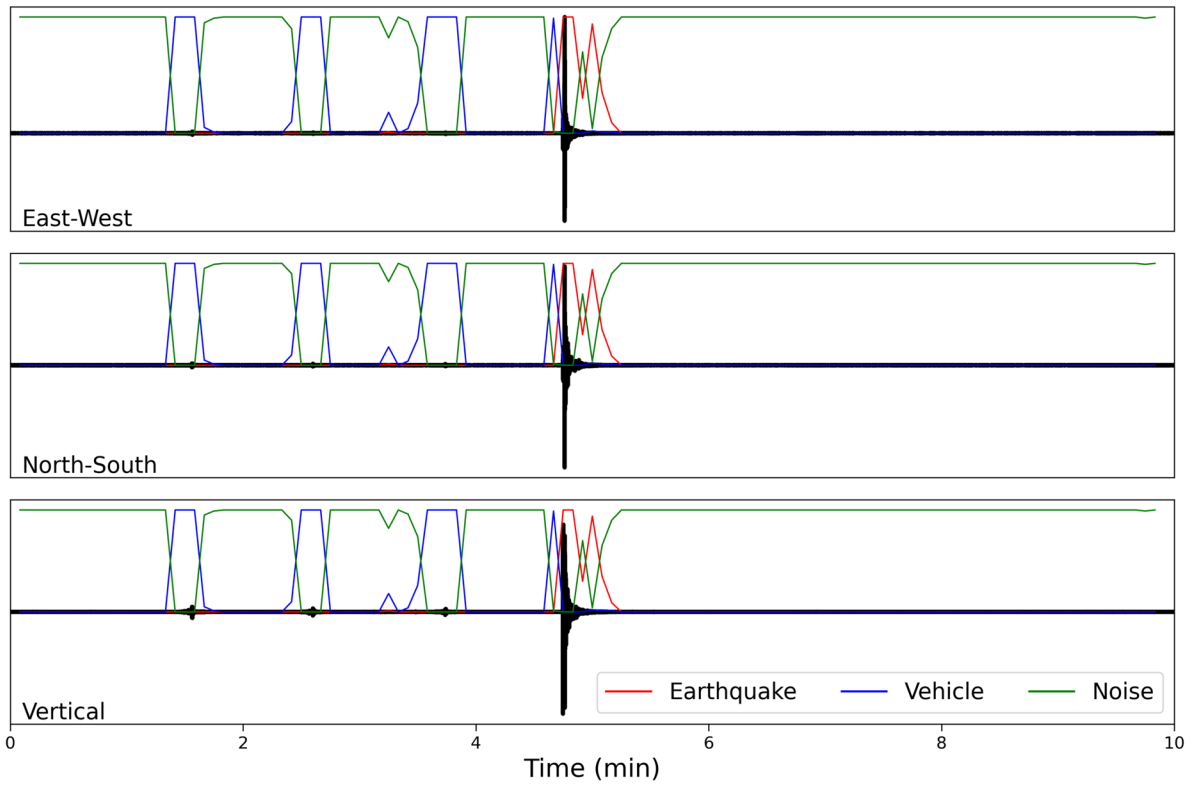

Fig. 8 Seismic trace of PBN station recorded on 5th of January 2023 between 22:50 (UTC) and 23:00 (UTC). Red, blue, and green lines are the model predictions for earthquake, vehicle, and noise, respectively

if the detection of vehicles is more important for the user, this result might be unsatisfactory. The model is not developed solely for vehicle detection, and it should not be used for this purpose.

Overall, our model performs well in detecting vehicle traces and earthquake signals. However, there are several aspects to stress about the model's capabilities. First, the input size of the model makes it suitable only for local earthquakes. Regional and teleseismic events cover longer time spans on seismic traces, and the model is not trained to use such inputs. Second, even though the noise information is retrieved from two different datasets, it may not provide information on all types of noises. If the model is used for another study area, it should be retrained with the data collected from the area to produce more accurate results. Third, the model is trained with several thousand vehicle traces from 3 stations, which may not be suitable to generalize

Table 3 Model prediction for earthquakes from INSTANCE and ITACA databases

		INSTANCE	ITACA
		Earthquake	
Prediction	Noise	385	1074
	Earthquake	9615	8038
	Vehicle	0	27
	Accuracy (%)	95.15	87.95

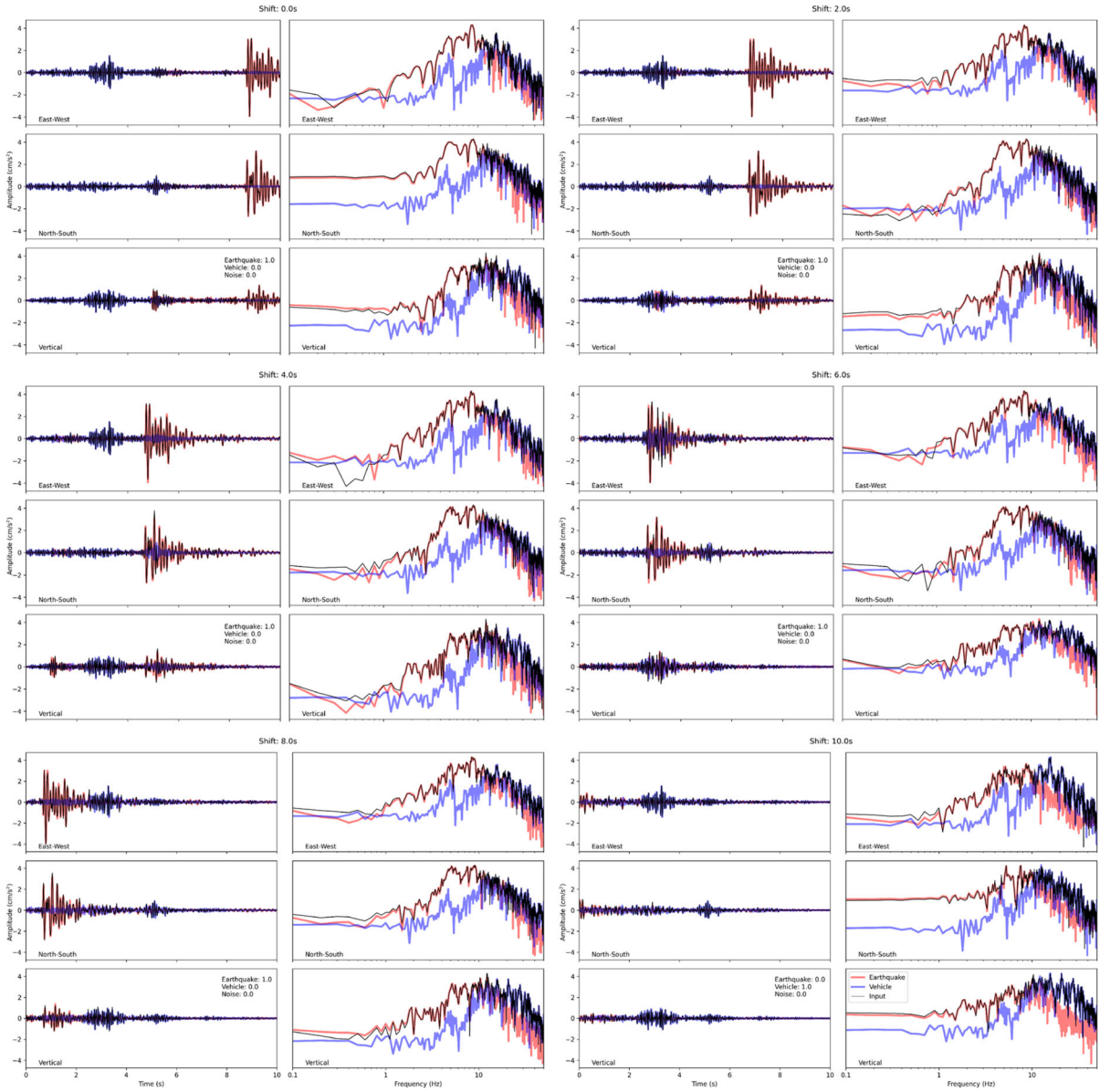

Fig. 9 Combined signal of the earthquake with shifted vehicle traces and their FFTs. Red, blue, and black colors present earthquake, vehicle, and combined trace, respectively. Model predictions for each class are given in the upper right side of the vertical component signal

all vehicle trace features. We do not know what type of vehicles passed near those stations. Hence, we may not have more specific types of vehicles. Furthermore, we do not use longer time spans in which the superposition of the multiple vehicle signals is recorded. However, the model can be improved by retraining with new vehicle traces to improve its detection capability. Moreover, input shapes and features can be rearranged depending on needs. Frequency-time information (e.g., short time Fourier transform, STFT can also be used instead of

FFT and might even be enough to separate the three classes as STFT can detect different seismic sources (Linville et al. 2019).

The developed model may predict the class of a given data in order of milliseconds. It is of vital importance when applied to real-time seismic monitoring. As explained in (Costa et al. 2022), seismic waveforms are constantly monitored for the RAN, and when a possible event is detected, FFTs of the waveforms with detection are automatically calculated. In this regard, our model requires no extra data processing step to be used in RAN routines and practically requires no extra processing power.

In this study, a machine learning algorithm is developed to detect three different features: noise, earthquake, and vehicle. To do that, visually labelled vehicle traces from 3 strong motion stations are used for vehicle class, whereas for earthquakes and noise classes, the STEAD database and RAN data are used. Seismic traces and frequency content are used to train a CNN network. The final model is selected from the best-performing model of 4 folds. The model is capable of predicting vehicles even with different datasets. Artificial data are created by superpositioning earthquake and vehicle traces to understand the limits of the network. In such a case, our model fails to detect the vehicle as it outputs earthquake class with high confidence. To understand the earthquake detection capabilities of the model, earthquake data coming from ITACA and INSTANCE databases are used. The model performs with high accuracy rates of 87.95 % and 95.15 % for the databases, respectively.

This study opens new perspectives for future studies on vehicle detection using seismic data. The effect of the superposition of vehicles can be analyzed in more detail. We do not consider the effect of attenuation, which influences the frequency content of vehicle signals. An extra layer of information should be collected to analyse such effects, such as visual evidence about the vehicles and their distance from the station.

Author contributions Conceptualisation, all authors.; methodology, D.E and A.D.L.; software, D.E and A.D.L.; data curation, D.E; writing–original draft preparation, D.E. and A.D.L.; writing–review and editing, all authors; visualisation, D.E. and A.D.L.; supervision, G.C.; project administration, G.C.; funding acquisition, G.C. All authors have read and agreed to the published version of the manuscript.

Funding Information This study received financial support from the Italian Civil Protection - Presidency of the Council of Ministers.

Code availability The datasets presented in this study can be found in GitHub (https://github.com/Machine-Learning-in-Seismology/Car-Detection).

Declarations

Competing interests The authors declare no competing interests.

References

Abadi M, Agarwal A, Barham P, Brevdo E, Chen Z, Citro C. Zheng X (2015) TensorFlow: Large-scale machine learning on heterogeneous systems. https://www.tensorflow.org/ (Software available from tensorflow.org)

Ahmad AB, Saibi H, Belkacem AN, Tsuji T (2022) Vehicle auto-classification using machine learning algorithms based on seismic fingerprinting. Computers 11(10):148. https://doi.org/10.3390/computers11100148

Allen RV (1978) Automatic earthquake recognition and timing from single traces. Bull Seismol Soc Am 68(5):1521–1532. https://doi.org/10.1785/BSSA0680051521

Bianchi I, Ruigrok E, Obermann A, Kissling E (2021) Moho topography beneath the european eastern alps by global-phase seismic interferometry. Solid Earth 12(5):1185–1196. https://doi.org/10.5194/se-12-1185-2021

Chollet F et al (2015) Keras. https://github.com/fchollet/keras. GitHub

Costa G, Brondi P, Cataldi L, Cirilli S, Ertuncay D, Falconer P, Turpaud P (2022) Near-real-time strong motion acquisition at national scale and automatic analysis. Sensors 22(15):5699. https://doi.org/10.3390/s22155699

Dou S, Lindsey N, Wagner AM, Daley TM, Freifeld B, Robertson M, Ajo-Franklin JB (2017) Distributed acoustic sensing

for seismic monitoring of the near surface: A traffic-noise interferometry case study. Sci Rep 7(1):11620. https://doi.org/10.1038/s41598-017-11986-4

Ertuncay D, Lorenzo A, Costa G (2024) Seismic signal discrimination of earthquakes and quarry blasts in North-East Italy using deep neural networks. Pure Appl Geophys 181(4):1139–1151. https://doi.org/10.1007/s00024-024-03440-0

Felicetta C, Russo E, D'Amico MC, Sgobba S, Lanzano G, Mascandola C, Luzi L (2023) Italian accelerometric archive (itaca), version 4.0. Istituto Nazionale di Geofisica e Vulcanologia (INGV). https://itaca.mi.ingv.it/ItacaNet_40/

Gallo A, Costa G, Suhadolc P (2014) Near real-time automatic moment magnitude estimation. Bull Earthquake Eng 12(1):185–202. https://doi.org/10.1007/s10518-013-9565-x

Ghofrani H, Atkinson GM, Schultz R, Assatourians K (2019) Short-term hindcasts of seismic hazard in the Western Canada Sedimentary Basin caused by induced and natural earthquakes. Seismol Res Lett 90(3):1420–1435. https://doi.org/10.1785/0220180285

Ghosh R, Akula A, Kumar S, Sardana H (2015) Time-frequency analysis based robust vehicle detection using seismic sensor. J Sound Vib 346:424–434. https://doi.org/10.1016/j.jsv.2015.02.011

Glorot X, Bengio Y (2010) Understanding the difficulty of training deep feedforward neural networks. Proceedings of the thirteenth international conference on artificial intelligence and statistics, pp 249–256

Gorini A, Nicoletti M, Marsan P, Bianconi R, de Nardis R, Filippi L, Zambonelli E (2010) The Italian strong motion network. Bull Earthquake Eng 8:1075–1090. https://doi.org/10.1007/s10518-009-9141-6

Gulia L, Gasperini P (2021) Contamination of Frequency-Magnitude Slope (b-Value) by Quarry Blasts: An Example for Italy. Seismol Res Lett. https://doi.org/10.1785/0220210080

Hashima S, Saad MH, Hatano K, Rizk H (2023) Vehicle classification in intelligent transportation systems using deep learning and seismic data. 2023 IEEE international conference on intelligence and security informatics (isi), pp 1–6

Jakkampudi S, Shen J, Li W, Dev A, Zhu T, Martin ER (2020) Footstep detection in urban seismic data with a convolutional neural network. Lead Edge 39(9):654–660. https://doi.org/10.1190/tle39090654.1

Jin G, Ye B, Wu Y, Qu F (2018) Vehicle classification based on seismic signatures using convolutional neural network. IEEE Geosci Remote Sens Lett 16(4):628–632. https://doi.org/10.1109/LGRS.2018.2879687

Kalra M, Kumar S, Das B (2020) Seismic signal analysis using empirical wavelet transform for moving ground target detection and classification. IEEE Sens J 20(14):7886–7895. https://doi.org/10.1109/JSEN.2020.2980857

Kennett B, Engdahl E (1991) Traveltimes for global earthquake location and phase identification. Geophys J Int 105(2):429–465. https://doi.org/10.1111/j.1365-246X.1991.tb06724.x

Ketcham SA, Anderson TS, Lacombe J, Moran ML (2005) Seismic propagation from humans in open and urban terrain. 2005 users group conference (dod-ugc'05), pp 270–277

Köse E, Hocaoğlu AK (2023) Convlstm-based vehicle detection and localization in seismic sensor networks. IEEE Access 11:139306–139313. https://doi.org/10.1109/ACCESS.2023.3340986

Lacroix P, Grasso J-R, Roulle J, Giraud G, Goetz D, Morin S, Helmstetter A (2012) Monitoring of snow avalanches using a seismic array: Location, speed estimation, and relationships to meteorological variables. J Geophys Res Earth Surf 117(F1):. https://doi.org/10.1029/2011JF002106

Le Gonidec Y, Kergosien B, Wassermann J, Jaeggi D, Nussbaum C (2021) Underground traffic-induced body waves used to quantify seismic attenuation properties of a bimaterial interface nearby a main fault. J Geophys Res Solid Earth 126(8):e2021JB021759. https://doi.org/10.1029/2021JB021759

Linville L, Pankow K, Draelos T (2019) Deep learning models augment analyst decisions for event discrimination. Geophys Res Lett 46(7):3643–3651. https://doi.org/10.1029/2018GL081119

Liu H, Ma J, Xu T, Yan W, Ma L, Zhang X (2019) Vehicle detection and classification using distributed fiber optic acoustic sensing. IEEE Trans Veh Technol 69(2):1363–1374. https://doi.org/10.1109/TVT.2019.2962334

Lythgoe K, Loasby A, Hidayat D, Wei S (2021) Seismic event detection in urban singapore using a nodal array and frequency domain array detector: earthquakes, blasts and thunderquakes. Geophys J Int 226(3):1542–1557. https://doi.org/10.1093/gji/ggab135

Meng H, Ben-Zion Y, Johnson CW (2021) Analysis of seismic signals generated by vehicle traffic with application to derivation of subsurface q-values. Seismol Soc Am 92(4):2354–2363. https://doi.org/10.1785/0220200457

Michelini A, Cianetti S, Gaviano S, Giunchi C, Jozinović D, Lauciani V (2021) Instance-the italian seismic dataset for machine learning. Earth Syst Sci Data 13(12):5509–5544. https://doi.org/10.5194/essd-13-5509-2021

Min R, Chen Y, Wang H, Chen Y (2024) Das vehicle signal extraction using machine learning in urban traffic monitoring. IEEE Trans Geosci Remote Sens 62:1–10. https://doi.org/10.1109/TGRS.2024.3371052

Mousavi SM, Sheng Y, Zhu W, Beroza GC (2019) Stanford earthquake dataset (stead): A global data set of seismic signals for ai. IEEE Access 7:179464–179476. https://doi.org/10.1109/ACCESS.2019.2947848

Presidency of Counsil of Ministers - Civil Protection Department (1972) Italian strong motion network. International Federation of Digital Seismograph Networks. https://www.fdsn.org/networks/detail/IT/

Riahi N, Gerstoft P (2015) The seismic traffic footprint: Tracking trains, aircraft, and cars seismically. Geophys Res Lett 42(8):2674–2681. https://doi.org/10.1002/2015GL063558

Sharma N, Jairath AK, Singh B, Gupta A (2012) Detection of various vehicles using wireless seismic sensor network. 2012 international conference on advances in mobile network, communication and its applications, pp 149–155

Sun L, Zhang Z, Tang H, Liu H, Li B (2023) Vehicle acoustic and seismic synchronization signal classification using long-term features. IEEE Sens J 23(10):10871–10878. https://doi.org/10.1109/JSEN.2023.3263572

Suriñach E, Vilajosana I, Khazaradze G, Biescas B, Furdada G, Vilaplana J (2005) Seismic detection and characteri-

zation of landslides and other mass movements. Nat Hazards Earth Syst Sci 5(6):791–798. https://doi.org/10.5194/nhess-5-791-2005

Uttarakumari M, Koushik AS, Raghavendra AS, Adiga AR, Harshita P (2017) Vehicle detection using acoustic signatures. 2017 international conference on computing, communication and automation (iccca), pp 1173–1177

Vičič B, Aoudia A, Javed F, Foroutan M, Costa G (2019) Geometry and mechanics of the active fault system in western slovenia. Geophys J Int 217(3):1755–1766. https://doi.org/10.1093/gji/ggz118

Wang Q, Zheng J, Xu H, Xu B, Chen R (2017) Roadside magnetic sensor system for vehicle detection in urban environments. IEEE Trans Intell Transp Syst 19(5):1365–1374. https://doi.org/10.1109/TITS.2017.2723908

Wang Y, Cheng X, Zhou P, Li B, Yuan X (2019) Convolutional neural network-based moving ground target classification using raw seismic waveforms as input. IEEE Sens J 19(14):5751–5759. https://doi.org/10.1109/JSEN.2019.2907051

Withers M, Aster R, Young C, Chael E (1996) High-frequency analysis of seismic background noise and signal-to-noise ratio near datil, new mexico. Bull Seismol Soc Am 86:1507–1515. https://doi.org/10.1785/BSSA0860051507

Yuan S, Liu J, Noh HY, Clapp R, Biondi B (2024) Using vehicle-induced das signals for near-surface characterization with high spatiotemporal resolution. J Geophys Res Solid Earth 129(4):e2023JB028033. https://doi.org/10.1029/2023JB028033. https://agupubs.onlinelibrary.wiley.com/doi/abs/10.1029/2023JB028033 (e2023JB028033 2023JB028033) https://agupubs.onlinelibrary.wiley.com/doi/pdf/10.1029/2023JB028033

Zambonelli E, de Nardis R, Filippi L, Nicoletti M, Dolce M (2011) Performance of the Italian strong motion network during the 2009, L'Aquila seismic sequence (central Italy). Bull Earthquake Eng 9:39–65. https://doi.org/10.1007/s10518-010-9218-2

Zhao Y, Rector JW (2010) Using seismic surface waves generated by motor vehicles to find voids: Field results. Seg technical program expanded abstracts 2010, pp 2029–2033. Society of Exploration Geophysicists

Zhu X, Zhang J, Zhang J (2023) Identification of vehicles from seismic signals using machine learning, vol All Days. https://doi.org/10.1190/image2023-3914280.1